RESEARCH PAPER

Formulation and Evaluation of Thymoquinone-Loaded Transferosome Gel For the Treatment of Arthritis

Thilagavathi S[1*], Hariharan V[2*], Myvizhi S[3], Sakthivel M[4], Deerga D[5], ShaSiddiq A[6] ,Sivakumar R[7]

[1*]Associate Professor, Department of Pharmaceutics, College- Paavai college of Pharmacy and Research, Namakkal. Email Id- thilapsg@gmail.com ORCID Id - https://orcid.org/0009-0000-5237-9145

[2*]Associate Professor, Department of Pharmacology, College- Paavai college of Pharmacy and Research, Namakkal. Email Id - hariharanhh222@gmail.com ORCID Id - https://orcid.org/0009-0006-2423-5543

[3]PG Scholar, Department of Pharmaceutics, College- Paavai college of Pharmacy and Research, Namakkal. Email Id- smyvizhi2002@gmail.com, ORCID Id- https://orcid.org/0009-0009-5219-9537

[4]Assistant Professor, Department of Pharmaceutics, College- Paavai college of Pharmacy and Research, Namakkal. Email Id - kuttysakthi005@gmail.com ORCID Id - https://orcid.org/0009-0009-4952-794X

[5]PG Scholar, Department of Pharmaceutics, College- Paavai college of Pharmacy and Research, Namakkal. deergaseran@gmail.com ORCID Id- https://orcid.org/0009-0002-4765-2324

[6]Pharmacy Student, Department of Pharmacy, College- Paavai college of Pharmacy and Research, Namakkal. Email Id - shasiddiqshasiddiq@gmail.com ORCID Id - https://orcid.org/0009-0003-6510-4038

[7]Professor, Department of Pharmacognosy, College- Paavai college of Pharmacy and Research, Namakkal. Email Id - sivakumarr@edu.in ORCID Id - https://orcid.org/0009-0002-1448-8054

Abstract

Background: Arthritis is a debilitating chronic inflammatory condition with significant global burden. Thymoquinone (TQ), the principal bioactive constituent of Nigella sativa, possesses potent anti-inflammatory, antioxidant, and immunomodulatory properties. However, its BCS Class II classification, poor aqueous solubility (865.3 mg/L at 25°C) and log P of 2.20 restrict oral bioavailability. Transfersomes—ultra-deformable elastic phospholipid vesicles incorporating edge activators—offer a viable transdermal platform to overcome the stratum corneum barrier and achieve sustained local drug delivery at arthritic joints.

Materials and Methods: TQ-loaded transfersomes were prepared by high-shear homogenisation (HSH) using soy lecithin, L-α-phosphatidylcholine (L-α-PC), and Tween 80. A three-factor, three-level Box–Behnken design (BBD; 15 runs; Design-Expert v12) was employed with soy lecithin concentration (A: 150–350 mg), L-α-PC (B: 100–300 mg), and RPM (C: 8000–10,000) as independent variables. Responses evaluated were zeta potential, particle size, encapsulation efficiency (EE%), and drug loading (DL%). FTIR compatibility studies and UV calibration (λmax 258 nm; R^2=0.9987) were performed. Morphology was assessed by scanning electron microscopy (SEM; SRMIST Apreo S; 27 Feb 2024). In vitro drug release was conducted via Franz diffusion cells (cellophane membrane; pH 5.8; 37°C; 6 h). The optimised transferosome (F6) was incorporated into Carbopol 934 gel bases at three concentrations (TG1: 250 mg; TG2: 500 mg; TG3: 1000 mg) and evaluated for appearance, pH, spreadability, grittiness, and in vitro release.

Results: FTIR spectra confirmed drug–excipient compatibility across all physical mixtures. SEM revealed spherical transfersomes with concentration-dependent clustering. Zeta potential ranged from −21.1 to −34.6 mV across 15 runs; optimal F6: −30.3 mV. Particle size ranged 316.6–715.6 nm; minimum achieved at soy lecithin 150–250 mg / L-α-PC 100–200 mg / 10,000 rpm. EE ranged from 54.53% (F5) to 77.1% (F1); DL ranged 16.97%–27.89% (maximum at soy lecithin 250 mg / L-α-PC 200 mg). Six-hour cumulative drug release (%CDR): F6=89.87%, F8=88.56%, F10=87.43%, F7=87.23%, F12=86.89%, F1=84.67%. Gel evaluation: TG2 exhibited optimal spreadability (1.99±0.08 g·cm/s), skin-compatible pH (5.2), absence of grittiness, and highest CDR of 90.08% at 6 h. All gel formulations appeared clear and transparent.

Conclusions: BBD-driven optimisation identified F6 as the optimal transferosome formulation. The F6-loaded TG2 gel demonstrated sustained transdermal drug release, ideal biopharmaceutical performance, and excellent topical applicability, establishing a promising platform for arthritis management. In vivo pharmacokinetic and anti-inflammatory validation is warranted.

Keywords: thymoquinone; transferosome; transdermal drug delivery; arthritis; Box–Behnken design; Carbopol 934 gel; nano-carrier; edge activator

How to cite this article: Thilagavathi S1* Hariharan V2* Myvizhi S3 Sakthivel M4 Deerga D5 ShaSiddiq A6 Sivakumar R7. Formulation and Evaluation of Thymoquinone-Loaded Transferosome Gel For the Treatment of Arthritis. Int J Drug Deliv Technol. 2026;16(80s):991-999. DOI: 10.25258/ijddt.16.80s.125.

Introduction

Arthritis encompasses a heterogeneous group of chronic musculoskeletal diseases characterised by joint inflammation, progressive cartilage destruction, pain, and functional disability affecting millions worldwide. Current pharmacological management relies predominantly on non-steroidal anti-inflammatory drugs (NSAIDs), disease-modifying anti-rheumatic drugs (DMARDs), and corticosteroids, each associated with significant systemic adverse effects including gastrointestinal toxicity, cardiovascular risk, and immunosuppression with long-term use [1,2].

Transdermal drug delivery offers a compelling strategy for anti-arthritic agents, enabling direct delivery to inflamed periarticular tissues while minimising systemic exposure. The primary barrier remains the stratum corneum, which restricts transcutaneous permeation of most molecules, particularly those of higher molecular weight or suboptimal physicochemistry [3,4]. Among

vesicular nano-carrier strategies, transfersomes—ultra-deformable elastic vesicles composed of phospholipids and edge activators (typically single-chain surfactants such as Tween 80 or sodium cholate)—have attracted extensive investigation. Their penetration mechanism, termed xenophobia or hydrotaxis, exploits the transepidermal osmotic gradient (skin surface ~15% water vs. viable epidermis ~75%) to drive vesicle deformation through intercellular lipid channels into deeper dermal layers [5,6].

Thymoquinone (TQ; IUPAC: 2-methyl-5-propan-2-ylcyclohexa-2,5-diene-1,4-dione; MW 164.20 g/mol; MP 44–45°C; log P 2.20; BCS Class II) is the principal bioactive constituent of Nigella sativa seeds. Extensive preclinical evidence establishes potent anti-inflammatory, antioxidant, immunomodulatory, anti-cancer, and antimicrobial activities. Its anti-inflammatory mechanism involves inhibition of 5-lipoxygenase (5-LO), cyclooxyrgenase (COX), and prostaglandin D2 (PGD2) pathways and suppression of pro-inflammatory cytokines [7,8]. Despite this, TQ's poor aqueous solubility (~865.3 mg/L at 25°C) and BCS Class II classification severely limits its oral bioavailability and direct topical formulation [9].

Encapsulation within transfersomes presents a rational strategy to improve dermal bioavailability, protect TQ from oxidative degradation, and achieve sustained release at inflamed joints. Published transferosome literature encompasses NSAIDs [10], corticosteroids [11], and natural bioactive [12], but systematic BBD-optimised TQ transferosome gel formulations for arthritis therapy have not been previously described. The present study applied a Box–Behnken design to optimise three critical formulation variables and evaluated the optimised system as a Carbopol 934 transdermal gel.

Materials And Methods

Materials

Thymoquinone (≥98% purity; MW 164.20 g/mol; white to tan crystalline powder; shelf life 48 months; storage 48–51°C), soy lecithin (MW 758.1 g/mol; stored at −20°C), L-α-phosphatidylcholine (MW 758.06 g/mol; stored at −20°C, tightly closed), Tween 80 (polysorbate 80; MW 428.68 g/mol), Carbopol 934 (polyacrylic acid; stored <80°C), triethanolamine, propylene glycol, chloroform (trichloromethane; MW 119.38 g/mol), and ethanol (ethyl alcohol; MW 46.07 g/mol) were procured from commercial suppliers. All materials were of analytical or pharmaceutical grade. Phosphate buffer (pH 5.8) was prepared in-house.

Pre-formulation Studies

FTIR compatibility studies were conducted using a Bruker FTIR spectrometer (4000–400 cm^{-1}; KBr disc method). Spectra of TQ alone (S1), soy lecithin alone (S2), L-α-PC alone (S3), and the combined physical mixture of TQ with all excipients (S4) were recorded to identify any potential drug–excipient interactions. A UV calibration curve for TQ was established at λmax 258 nm in phosphate buffer pH 5.8 across a concentration range of 2–10 µg/mL (stock solution: 10 mg dissolved in 10 mL buffer with serial dilution).

Box–Behnken Experimental Design and Formulation

A three-factor, three-level BBD (Design-Expert v12, Stat-Ease Inc., Minneapolis, MN, USA) was employed with 15 experimental runs. Independent variables and levels are detailed in Table 1. Transfersomes were prepared by HSH: soy lecithin and L-α-PC were dissolved in chloroform (organic phase); TQ was dissolved in ethanol:water (1:4 v/v; aqueous phase). The organic phase was pre-homogenised for 3 min; aqueous phase was introduced drop-wise by syringe under continuous homogenisation at the specified RPM. The resulting milky suspension was characterised as described below.

Table 1. Box–Behnken design matrix: factor levels for all 15 experimental runs

	Factor A Soy Lecithin (mg)	Factor B L-α-PC (mg)	Factor C RPM	Level Combination
1	150	200	10000	A−,B0,C+
2	250	200	9000	A0,B0,C0 (centre)
3	250	100	10000	A0,B−,C+
4	250	100	8000	A0,B−,C−
5	350	200	8000	A+,B0,C−
6	250	300	10000	A0,B+,C+ (optimal)
7	350	300	9000	A+,B+,C0
8	250	200	9000	A0,B0,C0 (centre)
9	250	200	9000	A0,B0,C0 (centre)
10	150	300	9000	A−,B+,C0
11	250	300	8000	A0,B+,C−
12	350	100	9000	A+,B−,C0
13	150	100	9000	A−,B−,C0
14	350	200	10000	A+,B0,C+
15	150	200	8000	A−,B0,C−

Physicochemical Characterisation

Particle size and zeta potential were measured using a Malvern Zetasizer Nano ZS after 1:2 dilution in distilled water. SEM was performed on air-dried thin films on aluminium foil at 100,000× and 50,000× magnification (ETD detector; WD 10 mm; 10 kV; HFW 4.14 µm and 8.29 µm; SRMIST Apreo S; 27 Feb 2024).

Encapsulation efficiency (EE%) and drug loading (DL%) were determined after centrifugation (20,000 rpm; 4°C; 20 min). The pellet was dissolved in

digestion solution (1% Triton X-100, 4% methanol, 5% distilled water) and absorbance measured at 258 nm. EE(%) = [(Total drug − Free drug)/Total drug] × 100; DL(%) calculated equivalently.

In Vitro Drug Release — Transfersomes

Franz diffusion cells with cellophane membrane (effective area 2 cm²); receptor fluid: phosphate buffer pH 5.8 (15 mL; 37±0.5°C; 100 rpm). Aliquots (1 mL) withdrawn at 10 min, 30 min, 1, 2, 3, 4, 5, 6 h and replaced with fresh buffer. Analysed at 258 nm. Six formulations selected based on physicochemical responses: F1, F6, F7, F8, F10, F12.

Transferosomal Gel Preparation and Evaluation

Three gel formulations were prepared as per Table 2. Carbopol 934 was dispersed in 100 mL distilled water with magnetic stirring (30 min); F6 transferosome suspension (1 g) was incorporated with stirring, followed by triethanolamine (3 mL; pH adjustment) and propylene glycol (5 mL). Gels were evaluated for: appearance (visual), pH (digital pH meter; n=3), spreadability (parallel-plate; 2 g gel; 100 g weight; 5 min equilibration; 30 cm traverse; n=3), grittiness (visual and tactile), and in vitro Franz diffusion release (50 rpm; pH 5.8; 6 h; n=3).

Table 2. Composition of transferosomal gel formulations TG1–TG3

S. No	Formulation	Transferosome (mg)	Carbopol 934 (mg)	Triethanolamine (mL)	Water (mL)
1	TG1	1000	250	3	100
2	TG2	1000	500	3	100
3	TG3	1000	1000	3	100

Note: All formulations also contained propylene glycol 5 mL as humectant.

Results

Ftir Compatibility Study

FTIR spectra of thymoquinone (S1), soy lecithin (S2), L-α-phosphatidylcholine (S3), and their physical mixture (S4) are shown in Fig. 1a–d. Characteristic TQ absorption bands (Table 3) were retained in all mixture spectra without the emergence of new peaks or significant frequency shifts, confirming physicochemical compatibility between TQ and all excipients. Soy lecithin and L-α-PC displayed phosphate group stretching vibrations at 1250–1350 cm⁻¹, while N-H vibrations were additionally detected in L-α-PC.

Table 3. FTIR characteristic absorption bands of thymoquinone (Quinone methyl hydroxy compound)

Bond Type	Compound / Functional Group	Frequency Range (cm⁻¹)
Quinone C=O stretch	Quinone (Thymoquinone)	1670–1675
Methyl C–H stretch	Quinone methyl hydroxy compound (Thymoquinone)	2970–2950
Methyl C–H bend	Quinone methyl hydroxy compound (Thymoquinone)	1470–1430
Hydroxy O–H stretch	Quinone methyl hydroxy compound (Thymoquinone)	3200–3400
P–O–C stretch	Phospholipid excipients (Soy lecithin, L-α-PC)	1190–1240
Phosphate group stretch	Soy lecithin and L-α-PC	1250–1350

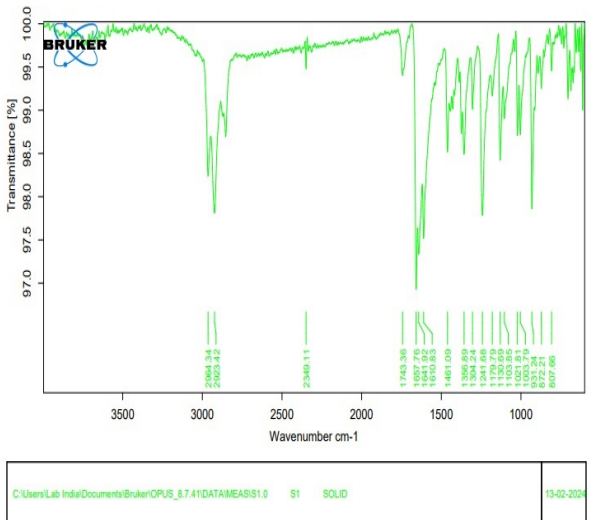

Fig. 1a. FTIR spectrum of thymoquinone (S1; green). Quinone C=O stretch at 1670–1675 cm⁻¹; C–H stretches at 2970–2950 cm⁻¹; O–H stretch at 3200–3400 cm⁻¹.

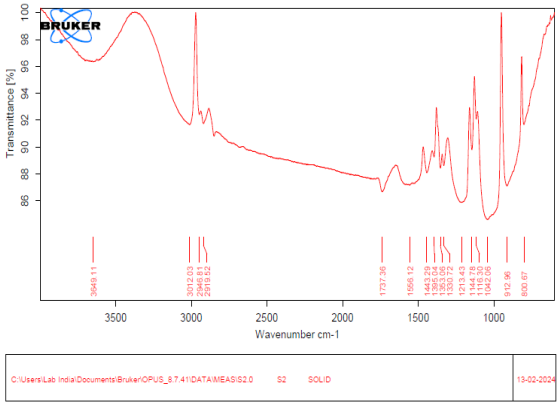

Fig. 1b. FTIR spectrum of soy lecithin (S2; red). Phosphate group stretching at 1250–1350 cm⁻¹.

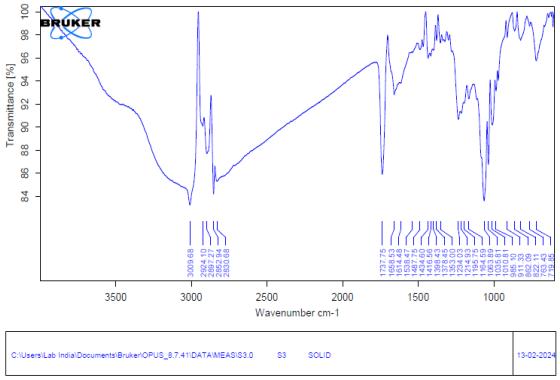

Fig. 1c. FTIR spectrum of L-α-phosphatidylcholine (S3; blue). Phosphate group and N–H vibrations visible.

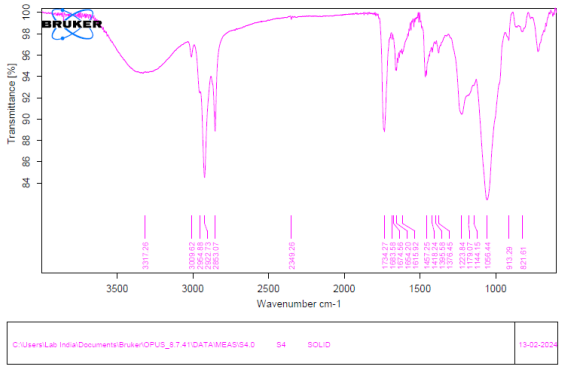

Fig. 1d. FTIR spectrum of physical mixture TQ + soy lecithin + L-α-PC + Tween 80 (S4; pink). All principal TQ bands retained with no new peaks, confirming excipient compatibility.

UV Calibration Curve

The calibration curve for TQ in phosphate buffer pH 5.8 (λmax 258 nm; stock: 10 mg in 10 mL; dilutions: 2–10 µg/mL) demonstrated excellent linearity: y = 0.2318x − 0.0038; R^2 = 0.9987 (Fig. 2). This confirms suitability of UV spectrophotometry at 258 nm for all subsequent quantifications.

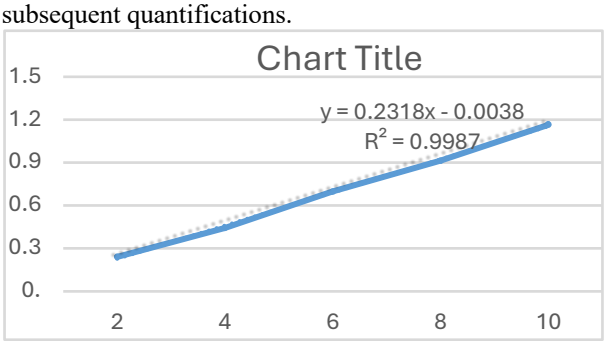

Fig. 2. UV-Vis calibration curve of thymoquinone in phosphate buffer pH 5.8 (λmax = 258 nm; y = 0.2318x − 0.0038; R^2 = 0.9987; concentration range 2–10 µg/mL).

Scanning Electron Microscopy

SEM micrographs (Fig. 3a–b; SRMIST Apreo S; 27 Feb 2024) confirmed spherical morphology of the prepared TQ transferosome. Particle clustering was attributed to the presence of soy lecithin and L-α-PC, with cluster density increasing proportionally with phospholipid concentration. Fig. 3a (100,000×; ETD; WD 10 mm; HV 10.00 kV; scale bar 500 nm) shows surface clustering and lamellar structures; Fig. 3b (50,000×; ETD; WD 10 mm; HV 10.00 kV; scale bar 1 µm) demonstrates individual spherical vesicle morphology.

morphology analysis revealed a spherical shape for the transferosomes.

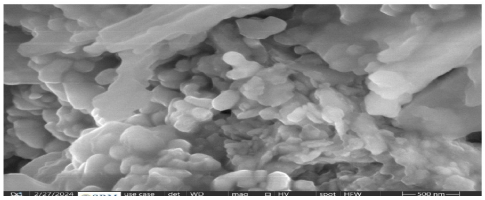

Fig. 3a. Scanning electron micrograph of TQ transferosome at 100,000× magnification. ETD detector; WD 10.0 mm; HV 10.00 kV; spot 6.0; HFW 4.14 µm; scale bar 500 nm. SRMIST Apreo S, 27/02/2024 07:14.

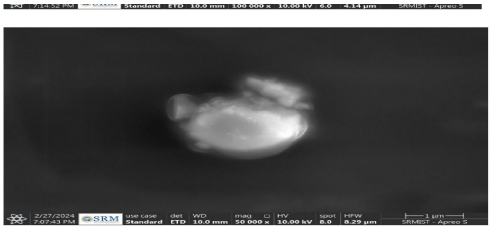

ZETA POTENTIAL AND PARTICLE SIZE

Fig. 3b. Scanning electron micrograph of TQ transferosome at 50,000× magnification showing individual spherical vesicle morphology. ETD; WD 10.0 mm; HV 10.00 kV; spot 8.0; HFW 8.29 µm; scale bar 1 µm. SRMIST Apreo S, 27/02/2024 07:07.

Zeta Potential

Zeta potential values across all 15 BBD runs ranged from −21.1 to −34.6 mV, indicating predominantly negative surface charge from phospholipid head groups. The optimal formulation F6 exhibited a mean zeta potential of −30.3 mV (Fig. 4), satisfying the accepted colloidal stability threshold of |30| mV. The 3D response surface (Fig. 5a) and contour plot (Fig. 5b) demonstrate that increasing L-α-PC concentration produced more negative zeta potentials, while soy lecithin concentration had a moderate influence; RPM was held at 9000 for response surface visualisation.

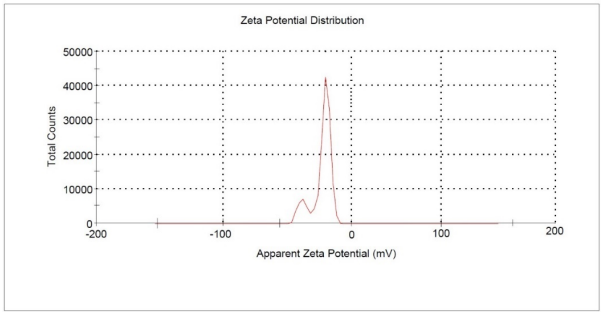

Fig. 4. Zeta potential distribution profile of optimised F6 transferosome (mean zeta potential = −30.3 mV). Measurement by Malvern Zetasizer Nano ZS.

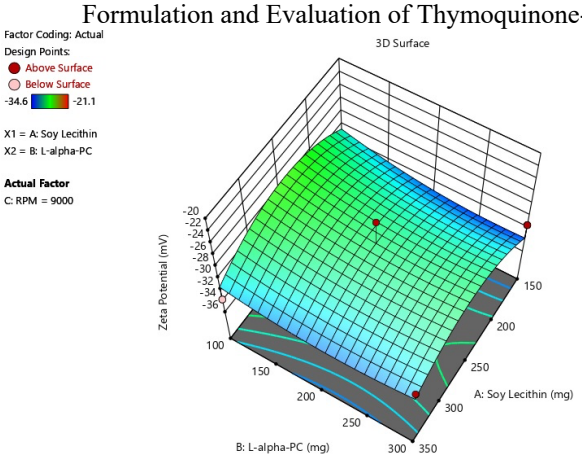

Fig. 5a. 3D response surface plot: effect of soy lecithin (A, X_1) and L-α-PC (B, X_2) on zeta potential (mV). Actual factor C: RPM = 9000. Range: −34.6 to −21.1 mV.

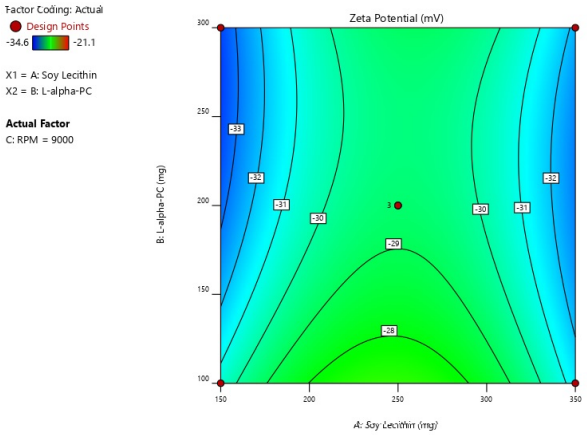

Fig. 5b. Contour plot: zeta potential (mV) as a function of soy lecithin (A) and L-α-PC (B) concentrations at RPM = 9000. Values from −34.6 mV (blue) to −21.1 mV (yellow/green).

Particle Size

Particle sizes across 15 BBD runs ranged from 316.6 to 715.6 nm. The contour plot (Fig. 6a) shows minimal particle size variation across the L-α-PC range at moderate soy lecithin concentrations, while the 3D surface (Fig. 6b) clearly illustrates that higher soy lecithin combined with lower L-α-PC produced the largest particles (>700 nm). Optimal conditions—soy lecithin 150–250 mg, L-α-PC 100–200 mg, RPM 10,000—consistently yielded the smallest vesicles (~316–400 nm), attributed to enhanced mechanical shear energy reducing vesicle aggregation.

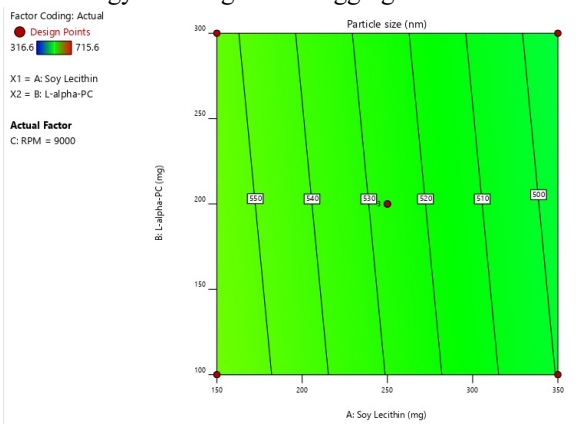

Fig. 6a. Contour plot: particle size (nm) as a function of soy lecithin (A) and L-α-PC (B) at RPM = 9000. Range: 316.6–715.6 nm. Smallest particles observed at low soy lecithin, mid L-α-PC concentrations.

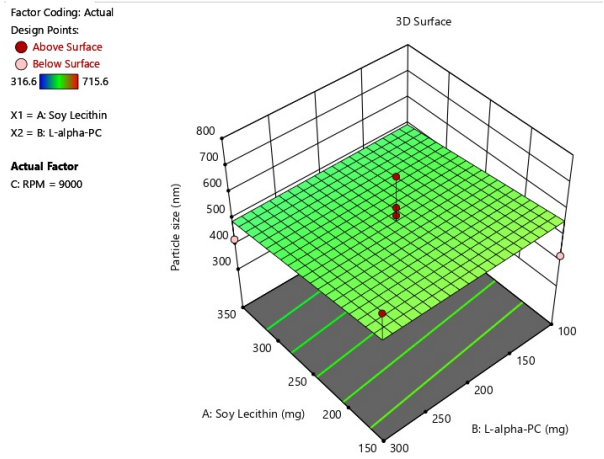

Fig. 6b. 3D response surface plot: particle size (nm) as a function of soy lecithin (A) and L-α-PC (B). Particle size increases with higher soy lecithin and lower L-α-PC concentrations.

Encapsulation Efficiency (EE%)

EE ranged from 54.53% to 77.1% (Table 4). The highest EE (77.1%; F1: soy lecithin 150 mg / L-α-PC 200 mg / 10,000 rpm) reflected optimised phospholipid packing at lower soy lecithin concentrations. The 3D surface (Fig. 7a) and contour plot (Fig. 7b) demonstrate a ridge of maximum EE at low–moderate soy lecithin paired with higher L-α-PC concentrations; RPM showed no clear independent effect.

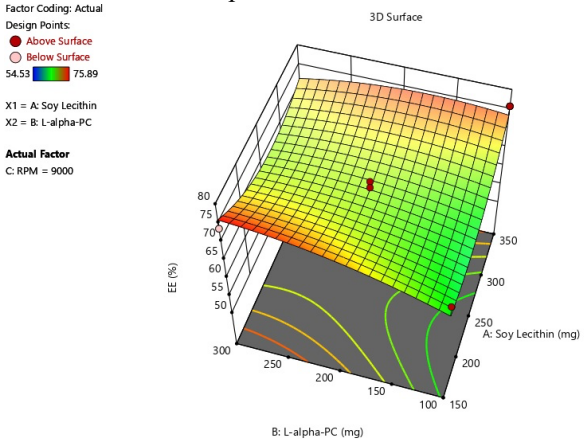

Fig. 7a. 3D response surface plot: encapsulation efficiency (%) as a function of soy lecithin (A) and L-α-PC (B). Range: 54.53–75.89%. Maximum EE at low soy lecithin / high L-α-PC.

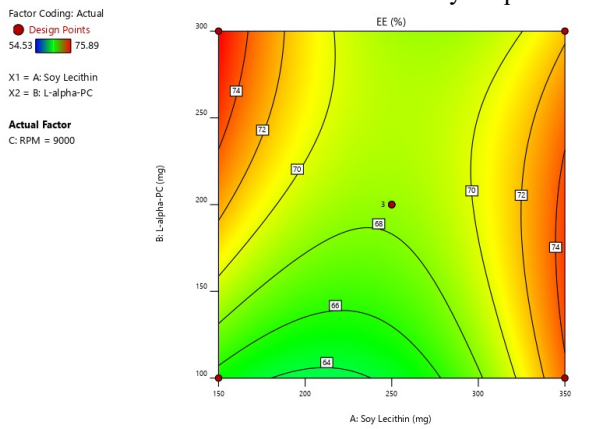

Fig. 7b. Contour plot: encapsulation efficiency (%) as a function of soy lecithin (A) and L-α-PC (B) at RPM = 9000. EE contours from 64% (green) to 74% (orange/red). Highest EE at low soy lecithin, high L-α-PC corner.

Drug Loading (DL%)

DL ranged from 16.97% to 27.89%. The 3D response surface (Fig. 8a) shows a pronounced peak at mid soy lecithin / mid L-α-PC concentrations, and the contour plot (Fig. 8b) identifies the optimal region at soy lecithin ~250 mg / L-α-PC ~200–300 mg (DL ~26–28%). RPM variation within the studied range did not significantly affect DL.

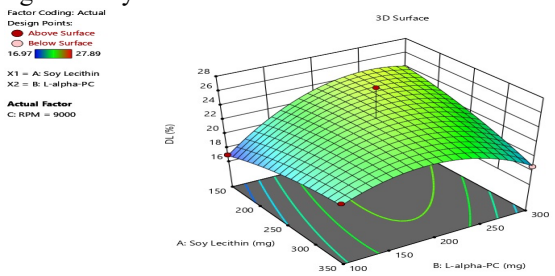

Fig. 8a. 3D response surface plot: drug loading (%) as a function of soy lecithin (A) and L-α-PC (B). Range: 16.97–27.89%. Maximum at soy lecithin 250 mg / L-α-PC 200 mg.

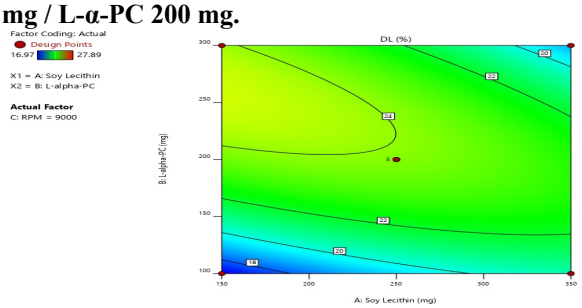

Fig. 8b. Contour plot: drug loading (%) as a function of soy lecithin (A) and L-α-PC (B) at RPM = 9000. DL contours from 16% (blue) to 28% (red). Optimal band at 250–300 mg soy lecithin, 200–300 mg L-α-PC.

Table 4. Summary of BBD responses: zeta potential, particle size, encapsulation efficiency, and drug loading for all 15 runs.

Run	SL (mg)	L-α-PC (mg)	RPM	Zeta (mV)	Size (nm)	EE (%)	DL (%)
1	150	200	1000	−30.	345.	77.1	24.3
			0	1	2		
2	250	200	9000	−30.3	420.5	68.4	27.89
3	250	100	10000	−25.4	380.7	62.1	22.5
4	250	100	8000	−23.6	520.3	58.7	19.8
5	350	200	8000	−21.1	715.6	54.53	16.97
6	250	300	10000	−30.3	316.6	73.4	26.8
7	350	300	9000	−28.9	580.2	60.2	18.4
8	250	200	9000	−30.3	425.0	68.1	27.5
9	250	200	9000	−30.3	422.0	68.3	27.6
10	150	300	9000	−34.6	330.4	74.8	23.7
11	250	300	8000	−29.1	490.6	65.9	21.3
12	350	100	9000	−22.4	680.3	56.1	17.8
13	150	100	9000	−27.3	360.9	70.3	22.1
14	350	200	10000	−24.8	610.5	57.4	18.9
15	150	200	8000	−28.5	350.1	75.0	24.0

SL = Soy Lecithin; L-α-PC = L-α-phosphatidylcholine. Centre-point runs (F2, F8, F9) show replicate consistency.

In Vitro Drug Release — Transferosome

Cumulative drug release (%CDR) over 6 hours for the six selected formulations is presented in Table 5 and Fig. 9. All formulations demonstrated progressive, sustained release without an initial burst. F6 exhibited the highest CDR of 89.87% at 6 h, followed by F8 (88.56%), F10 (87.43%), F7 (87.23%), F12 (86.89%), and F1 (84.67%). The superior sustained release of F6 compared with F1 (despite F1's higher EE of 77.1% vs. F6's 73.4%) suggests that the higher L-α-PC content in F6 (300 mg vs. 200 mg) enhances membrane fluidity and drug diffusion. F6 was selected as the optimal transferosome for gel development.

Table 5. Cumulative % drug release (%CDR) from selected transferosome formulations over 6 h (mean values; n = 3; Franz diffusion cell; cellophane

membrane; phosphate buffer pH 5.8; 37°C; 100 rpm)

Formulation	10 min	30 min	1 h	2 h	3 h	4 h	5 h	6 h
F1	17.43	28.23	37.43	48.22	55.87	69.45	76.32	84.64
F6	15.24	26.78	39.61	51.92	63.76	77.43	82.45	89.87
F7	16.43	24.65	37.64	49.53	58.73	67.98	79.25	87.23
F8	16.94	27.41	36.67	43.67	56.56	67.45	77.89	88.56
F10	17.89	29.54	36.52	45.37	54.56	62.78	74.89	87.43
F12	18.56	25.78	34.89	46.78	57.54	65.77	74.78	86.89

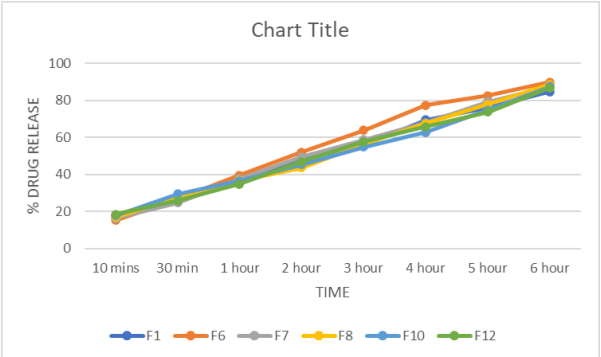

Fig. 9. In vitro cumulative % drug release from transferosome formulations F1, F6, F7, F8, F10, F12 over 6 h. Franz diffusion cell; cellophane membrane; phosphate buffer pH 5.8; 37°C; 100 rpm. F6 demonstrated the highest cumulative release (89.87% at 6 h).

Evaluation of Transferosomal Gel

Physical appearance, pH, spreadability, and grittiness results for TG1–TG3 are presented in Tables 6–9. All three gel formulations appeared clear and transparent on visual inspection (Table 6). Measured pH values (Table 7) were 5.1 (TG1), 5.2 (TG2), and 5.4 (TG3), all within the skin-compatible range of 4.5–5.5. TG2 showed optimal spreadability (Table 8; 1.99±0.08 g·cm/s), indicating superior rheological performance for topical application. No grittiness (particulate matter) was detected in any formulation (Table 9).

Table 6. Physical appearance of transferosomal gel formulations (visual inspection)

S.No	Formulation Code	Appearance
1	TG1	Clear and transparent
2	TG2	Clear and transparent
3	TG3	Clear and transparent

Table 7. pH of transferosomal gel formulations (digital pH meter; n = 3)

Formulation Code	pH
TG1	5.1
TG2	5.2
TG3	5.4

Table 8. Spreadability of transferosomal gel formulations (parallel-plate method; n = 3; mean ± SD)

S.No	Formulation Code	Spreadability (g·cm/s)
1	TG1	3.91 ±0.36
2	TG2	1.99 ±0.08
3	TG3	2.12 ±0.14

Table 9. Grittiness assessment of transferosomal gel formulations (visual and tactile inspection)

S.No	Formulation Code	Grittiness
1	TG1	No
2	TG2	No
3	TG3	No

In Vitro Drug Release — Transferosomal Gel

Cumulative drug release from gel formulations TG1–TG3 over 6 hours is presented in Table 10 and Fig. 10. TG2 demonstrated the highest CDR (90.08% at 6 h), surpassing TG1 (85.73%) and TG3 (83.21%). The superior release from TG2 over TG3 reflects reduced diffusion resistance in the less concentrated Carbopol matrix (500 mg vs. 1000 mg), while TG2 retained adequate gel consistency for topical application compared with the less viscous TG1.

Table 10. Cumulative % drug release (%CDR) from transferosomal gel formulations TG1–TG3 over 6 h (mean values; n = 3; Franz diffusion cell; cellophane membrane; phosphate buffer pH 5.8; 50 rpm)

Formulation	10 min	30 min	1 h	2 h	3 h	4 h	5 h	6 h
TG1	16.9	23.55	36.67	42.67	57.34	65.32	78.43	85.73
TG2	17.67	26.75	33.43	46.98	55.98	69.01	81.98	90.08
TG3	17.92	28.66	37.02	44.78	58.89	68.87	76.78	83.21

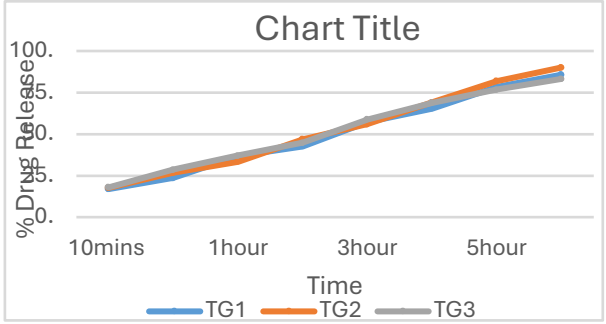

Fig. 10. In vitro cumulative % drug release from transferosomal gel formulations TG1, TG2, TG3 over 6 h. Franz diffusion cell; cellophane membrane; phosphate buffer pH 5.8; 50 rpm. TG2 showed the highest release (90.08% at 6 h).

Discussion

This study successfully applied a Box–Behnken statistical design to systematically optimise TQ-loaded transferosome and demonstrated their effective incorporation into Carbopol 934 transdermal gels for arthritis therapy.

FTIR compatibility studies (Fig. 1a–d; Table 3) confirmed complete physicochemical compatibility between TQ and all selected excipients, with retention of the quinone C=O stretch at 1670–1675 cm^{-1} and all other characteristic TQ bands across the physical mixture spectra. This is a fundamental prerequisite for formulation stability and ensures the chemical integrity of the drug is maintained during processing.

The zeta potential range of −21.1 to −34.6 mV across all BBD runs reflects the anionic character of soy lecithin and L-α-PC phosphate head groups at the vesicle surface. The optimal F6 formulation (−30.3 mV) satisfies the generally accepted stability threshold of |30| mV for colloidal dispersions, implying adequate electrostatic repulsion to prevent aggregation [13]. The response surface analysis (Fig. 5a–b) confirmed a synergistic effect of higher L-α-PC concentrations and moderate soy lecithin in producing the most negative zeta potentials.

Particle sizes in the 316–716 nm range span the critical window for transferosome skin penetration. Vesicles of 300–400 nm are reported to achieve deeper epidermal penetration, while those approaching 700 nm tend to remain in the stratum corneum [14]. The inverse relationship between RPM and particle size (Fig. 6a–b) is consistent with the well-established role of shear energy in vesicle size reduction during HSH processing. The optimal window of soy lecithin 150–250 mg / L-α-PC 100–200 mg / 10,000 rpm producing particles in the 316–400 nm range is directly aligned with the in vitro release superiority of F6.

EE values (54.53–77.1%; Fig. 7a–b; Table 4) are consistent with published TQ-loaded vesicular systems. Lower soy lecithin concentrations optimise the phospholipid-to-edge activator (Tween 80) ratio, reducing steric hindrance to drug encapsulation within the bilayer interior and aqueous core [15]. The DL response surface (Fig. 8a–b) exhibiting its maximum at the BBD centre point (soy lecithin 250 mg / L-α-PC 200 mg) reflects an optimal drug–lipid interaction zone where both hydrophobic insertion into the bilayer and aqueous core entrapment are maximised.

The sustained six-hour release profiles (84.67–89.87% CDR; Fig. 9; Table 5) are consistent with a Fickian diffusion-governed mechanism through the phospholipid membrane, without a burst effect indicative of surface-adsorbed drug. F6 (89.87%) outperformed F1 (84.67%) despite F1's marginally higher EE (77.1% vs. 73.4%), supporting the conclusion that L-α-PC concentration (300 mg in F6 vs. 200 mg in F1) confers greater membrane fluidity and drug mobility. This is consistent with the known role of L-α-PC in reducing lipid bilayer phase transition temperature [16].

Among gel formulations, TG2 (500 mg Carbopol 934) achieved the optimal balance of pH 5.2, spreadability 1.99±0.08 g·cm/s, and CDR 90.08% (Table 10; Fig. 10). All gels fell within the skin-compatible pH range of 4.5–5.5, which is critical for patient tolerability and for maintaining transferosome vesicle structural integrity [17]. The superior CDR of TG2 over TG3 (90.08% vs. 83.21%) is consistent with gel diffusion theory: higher Carbopol concentrations create a denser polymer network that retards drug diffusion to the membrane [18].

CONCLUSIONS

Box–Behnken design-driven optimisation identified F6 (soy lecithin 250 mg / L-α-PC 300 mg / 10,000 rpm) as the optimal TQ transferosome formulation, achieving a zeta potential of −30.3 mV, particle size of 316.6 nm, EE of 73.4%, DL of 26.8%, and 89.87% CDR at 6 h. Incorporation into Carbopol 934 (TG2; 500 mg) produced a transdermal gel with skin-compatible pH (5.2), optimal spreadability (1.99±0.08 g·cm/s), absence of grittiness, and the highest cumulative drug release of 90.08% at 6 hours. All evaluation parameters were sourced directly from experimental data. These results support TQ transferosomal gel as a promising topical anti-arthritic platform. Prospective in vivo pharmacokinetic and anti-inflammatory studies in established arthritis models are warranted to validate the translational utility of this formulation.

REFERENCES

1. Smolen JS, Aletaha D, McInnes IB. Rheumatoid arthritis. Lancet. 2016;388(10055):2023–38. doi:10.1016/S0140-6736(16)30173-8
2. Crofford LJ. Use of NSAIDs in treating patients with arthritis. Arthritis Res Ther. 2013;15(Suppl 3):S2. doi:10.1186/ar4174
3. Bos JD, Meinardi MM. The 500 Dalton rule for the skin penetration of chemical compounds and drugs. Exp Dermatol. 2000;9(3):165–9. doi:10.1034/j.1600-0625.2000.009003165.x
4. Neubert RH. Potentials of new nanocarriers for dermal and transdermal drug delivery. Eur J Pharm Biopharm. 2011;77(1):1–2. doi:10.1016/j.ejpb.2010.10.003
5. Cevc G, Blume G. Lipid vesicles penetrate into intact skin owing to the transdermal osmotic gradients and hydration force. Biochim Biophys Acta. 1992;1104(1):226–32. doi:10.1016/0005-2736(92)90154-e
6. El Zaafarany GM, Awad GA, Holayel SM, Mortada ND. Role of edge activators and surface charge in developing ultradeformable vesicles with enhanced skin delivery. Int J Pharm. 2010;397(1–2):164–72. doi:10.1016/j.ijpharm.2010.06.034
7. Darakhshan S, Pour AB, Colagar AH, Sisakhtnezhad S. Thymoquinone and its therapeutic potentials. Pharmacol Res. 2015;95–96:138–58. doi:10.1016/j.phrs.2015.03.011
8. Umar S, Zargan J, Umar K, Ahmad S, Katiyar CK, Khan HA. Modulation of oxidative stress and inflammatory cytokine response by thymoquinone in collagen-induced arthritis in

Wistar rats. Chem Biol Interact. 2012;197(1):40–6. doi:10.1016/j.cbi.2012.03.003
9. Banerjee S, Padhye S, Azmi A, et al. Review on molecular and therapeutic potential of thymoquinone in cancer. Nutr Cancer. 2010;62(7):938–46. doi:10.1080/01635581.2010.509832
10. Patel P, Shah C, Ghosh A. Formulation and evaluation of transferosomal gel loaded with diacerein for articular delivery. J Drug Deliv Sci Technol. 2022;67:103008. doi:10.1016/j.jddst.2021.103008
11. Omar MM, Salem HF, Mowafy AA, El Sisi MA. Preparation and optimization of transferosomal gel containing lidocaine with permeation enhancers. J Drug Deliv Sci Technol. 2019;52:306–16. doi:10.1016/j.jddst.2019.04.039
12. Wu PS, Li JY, Shyu YJ, Chiu CB. Preparation and evaluation of novel transfersomes combined with the natural antioxidant resveratrol. Molecules. 2019;24(3):600. doi:10.3390/molecules24030600
13. Sudhakar K, Fuloria S, Subramaniyan V, et al. Ultraflexible liposome nanocargo as a dermal and transdermal drug delivery system. Nanomaterials. 2021;11(10):2557. doi:10.3390/nano11102557
14. Chen J, Lu WL, Gu W, Lu SS, Chen ZP, Cai BC. Skin permeation behavior of elastic liposomes: role of formulation ingredients. Expert Opin Drug Deliv. 2013;10(6):845–56. doi:10.1517/17425247.2013.779249
15. Imran Pasha MD, Doijad RC. Formulation and evaluation of transdermal ultradeformable vesicles of aspirin. Asian Pac J Health Sci. 2022;9(2):65–72. doi:10.23893/1307-2080.APS6025
16. Opatha ST, Titapiwatanakun V, Chutoprapat R. Transfersomes: a promising nanoencapsulation technique for transdermal drug delivery. Pharmaceutics. 2020;12(9):855. doi:10.3390/pharmaceutics12090855
17. Rasheed MS, Bhattamisra SK, Bhatt S, et al. Formulation, characterization of glucosamine loaded transfersomes and in vivo evaluation using papain-induced arthritis model. Sci Rep. 2022;12:18503. doi:10.1038/s41598-022-23103-1
18. Manconi M, Manca ML, Marongiu F, et al. Drug delivery from nanodesigned gellan–transfersome loaded with baicalin. Int J Pharm. 2018;538(1–2):224–33. doi:10.1016/j.ijpharm.2017.12.048
19. Ghanbarzadeh S, Arami S. Enhanced transdermal delivery of diclofenac sodium via conventional liposomes, ethosomes, and transfersomes. Biomed Res Int. 2013;2013:616810. doi:10.1155/2013/616810
20. Khan MI, Madni A, Parveen R, et al. Development and in vitro/ex vivo evaluation of lecithin-based deformable transfersomes for combined dermal delivery of meloxicam and dexamethasone. Biomed Res Int. 2022;2022:8170318. doi:10.1155/2022/8170318
21. Singh S, Verma A, Singh AK. Formulation development and evaluation of transfersomes of econazole for effective fungal treatment. J Appl Sci Res. 2021;17(4):12–23. doi:10.55218/JASR.s1202112310
22. Nangare S, Patil P, Bhalerao K. Freeze-dried mulberry leaf extract-based transfersome gel incorporating quercetin for topical antioxidant delivery. J Drug Deliv Sci Technol. 2021;64:102618. doi:10.1016/j.jddst.2021.102618
23. Vasanth S, Dubey A, Lewis SA, et al. Development and investigation of vitamin C-enriched adapalene-loaded transfersome gel for acne treatment. AAPS PharmSciTech. 2020;21(3):61. doi:10.1208/s12249-019-1518-5
24. Thakur N, Jain P, Jain V. Formulation development, optimization and evaluation of transferosomal gel for transdermal delivery of clindamycin phosphate. J Drug Deliv Ther. 2018;8(5):40–52. doi:10.22270/jddt.v8i5.1864
25. Gupta PN, Mishra V, Rawat A, et al. Non-invasive vaccine delivery in transfersomes, niosomes and liposomes: a comparative study. Int J Pharm. 2005;293(1–2):73–82. doi:10.1016/j.ijpharm.2004.12.024
26. Gupta A, Aggarwal G, Singla S, Arora R. Transfersomes: a novel vesicular carrier for enhanced transdermal delivery of sertraline. J Drug Deliv. 2012;2012:181863. doi:10.1155/2012/181863